ADVANCED FUNCTIONAL MATERIALS
www.afm-journal.de

Highly Efficient TADF OLEDs: How the Emitter–Host Interaction Controls Both the Excited State Species and Electrical Properties of the Devices to Achieve Near 100% Triplet Harvesting and High Efficiency

Vygintas Jankus, Przemyslaw Data, David Graves, Callum McGuinness, Jose Santos, Martin R. Bryce, Fernando B. Dias, and Andrew P. Monkman*

New emitters that can harvest both singlet and triplet excited states to give 100% internal conversion of charge into light, are required to replace Ir based phosphors in organic light emitting diodes (OLEDs). Molecules that have a charge transfer (CT) excited state can potentially achieve this through the mechanism of thermally activated delayed fluorescence (TADF). Here, it is shown that a D–A charge transfer molecule in the solid state, can emit not only via an intramolecular charge transfer (ICT) excited state, but also from exciplex states, formed between the molecule and the host material. OLEDs based on a previously studied D–A–D molecule in a host TAPC achieves >14% external electroluminescence yield and shows nearly 100% efficient triplet harvesting. In these devices, it is unambiguously established that the triplet states are harvested via TADF, but more interestingly, these results are found to be independent of whether the emitter is the ICT state or the D–A–D/host exciplex.

1. Introduction

Artificial lighting is an essential part of our lives, which consumes 19% of the planet's electricity usage, and cheaper ways of creating energy, and more efficient devices that use less electricity, are needed to reduce energy costs, and greatly cut CO_2 production. Ultra-efficient lighting will play an important role in achieving this. In particular, white organic light emitting diodes (OLEDs) could become an integral part of the new lighting technologies; however, alternatives to Ir based phosphors, and especially much improved deep blue OLED emitters, are needed in order to give high quality, efficient white OLEDs that are not reliant on scarce rare-earth metals.

Two types of excited states are created when charge recombines in an OLED—singlet and triplet excitons—but only the singlets directly give light, which fundamentally limits external OLED efficiency to 5%.[1] Thus the efficiency can be increased fourfold if the non-emissive triplets can be utilised. Currently, phosphorescent heavy metal complexes are used to "harvest" the triplet states and generate light.[2–4] Unfortunately, pushing the metal-to-ligand charge transfer excited state of these complexes into the blue opens a non-radiative pathway via the metal d-orbitals, which limits efficiency,[5] and makes the complexes thermally and photochemically unstable.[6] The production of singlets via triplet–triplet annihilation (TTA), that is, triplet fusion (TF), has also been demonstrated in OLEDs,[7,8] but it has been shown that triplet annihilation can contribute to both an increase and a loss in yield in OLEDs,[9] and the maximum theoretical external quantum efficiency (EQE) 12.5%, when accounting for emission arising from TF, has not been reached. However, deep blue emission is essential to achieve the required colour rendering and efficiency in white OLEDs for lighting applications, therefore, other processes that can convert triplets to singlets must be found.

An alternative way to convert triplets to singlets in OLEDs has recently been reported by Adachi et al.[10,11] using thermally activated delayed fluorescence (TADF). In this case, emitters with a small electron exchange energy (singlet-triplet splitting) enable triplets to undergo thermally activated reverse intersystem crossing (rISC) to the singlet manifold[12,13] which could be a key solution for deep blue OLEDs. TADF OLEDs also have the advantages of intrinsically low turn on voltage and a very simple device structure, in many cases without an ambipolar host. This gives high power efficiency, crucial for lighting, and higher yields for large-area manufacturing.

Dr. V. Jankus, Dr. P. Data, D. Graves, C. McGuinness, Dr. F. B. Dias, Prof. A. P. Monkman
Physics Department, University of Durham
South Road, Durham DH1 3LE, UK
E-mail: vygintas.jankus@gmail.com
Dr. P. Data
Faculty of Chemistry
Silesian University of Technology
M. Strzody 9 44–100, Gliwice, Poland
Dr. J. Santos, Prof. M. R. Bryce
Department of Chemistry
University of Durham
South Road, Durham DH1 3LE, UK

DOI: 10.1002/adfm.201400948

Table 1. **2d**:TAPC OLED characteristics at various **2d** concentrations at 100 cd/m^2 and 1000 cd/m^2.

2d	Brightness [cd/m^2]	EQE [%]	Power Efficiency [lm/W]	Current Efficiency [cd/A]
5%	100	3.0	3.4	6.1
30%	100	10.3	26.7	32.3
38%	100	14.03	20.3	26.3
40%	100	13.8	25.7	31.1
50%	100	11.0	14.3	17.6
5%	1000	–	–	–
30%	1000	7.1	14.8	22.5
38%	1000	6.5	9.8	17.9
40%	1000	5.4	10.0	16.2
50%	1000	6.0	6.4	10.3

However, despite the fact that TADF has been shown to give highly efficient OLEDs,[14,15] the underlying mechanisms are still not clearly understood. For example, we have recently shown that the TADF mechanism in donor–acceptor (D–A) molecules is not as obvious as previously thought and that the n–π^* state may play a crucial role in the thermal activation step.[16a] We also have shown that TF in exciplex based OLEDs can compete with TADF leading to less efficient triplet recycling.[17] Another issue is the choice of an appropriate host having a high triplet level, similar to those used in phosphorescent devices.[18,19] It is therefore vital to understand the details of the TADF mechanism in solid state films and OLED devices, so that new more efficient materials sets can be designed for efficient blue TADF OLEDs in the future. Here we investigate the complicated dynamics of D–A–D TADF molecules in the solid state and in a host with a high triplet level in both film and devices. We observe the emission from three distinct excited states: i) local exciton (LE) state emission from the D–A–D molecule, ii) intramolecular charge transfer (ICT) emission again from the D–A–D molecule, and iii) emission from an exciplex formed between the D–A–D molecule and the host. We demonstrate that both CT states are very efficient, in harvesting up to 100% triplet excitons, and that the exciplex state yields OLED devices with external quantum efficiency >14%, even though the exciplex photoluminescence quantum yield is only 53%, corresponding to 50% internal efficiency and near 100% excited state harvesting.

2. Results and Discussions

2.1. OLED Studies

In our studies we have used the D–A–D molecule; 9-[2,8]-9-carbazole-[dibenzothiophene-*S*,*S*-dioxide]-carbazole (**2d**) and 4,4′-cyclohexylidenebis[*N*,*N*-bis(4-methylphenyl)benzenamine] (TAPC) host. . **2d** was chosen because it was demonstrated to have 100% triplet harvesting via TADF in solution, its photophysical properties in solution have been reported and TD-DFT calculations have been performed.[16a,b] We fabricated OLEDs having the following structure: ITO/NPB (60 nm)/ x% **2d**:TAPC (30 nm)/TPBi (10 nm)/BCP (20 nm)/LiF (1 nm)/Al, where x denotes the **2d** loading, either 5%, 30%, 38%, 40%, and 55% by weight. The highest EQE, 14.03%, (at 100 cd/m^2 luminance) was observed for 38% **2d** loading (**Table 1**). Devices with 30% **2d**:TAPC loading had the maximum values of luminous power efficiency and current efficiency at low luminance, that is, at 100 cd/m^2, 26.74 lm/W and 32.25 cd/A, respectively, and high luminance, that is, at 1000 cd/m^2, 14.82 lm/W and 22.47 cd/A. **Figure 1**a shows that all devices with high loadings of **2d** exhibit similar current–voltage characteristics. Clearly visible in all plots is the trap-controlled, space-charge limited conduction behaviour yielding a steep rise of current above 2.7 V turn-on.[20] Devices with increased **2d** content tend to exhibit lower leakage current densities at low bias, the current turn-on voltage of all four devices is close to the optical gap limit, 2.7 ± 0.05 V. The luminance turn-on voltages were similar for all devices at 2.75 ± 0.05 V, with the maximum luminance for 30% **2d** device of 4822 cd/m^2 at 8.0 V (Figure 1c). Devices containing 30%, 38% and 40% of **2d** exhibit a high 30 cd/A level of current efficiency and minimal roll-off up to 1000 cd/m^2 (Figure 1d). The very low drive voltage of these devices leads to a luminous power efficiency of >30 lm/W for the 40% **2d** device and >20 lm/W for all the high percentage **2d** devices (Figure 1f): this is an important factor for lighting applications.

In order to succinctly explain the excited state dynamics in these **2d**:TAPC systems, we will concentrate on describing the photophysics of films and OLEDs with 5% and 30% **2d** loadings. OLEDs with 30% loading demonstrated the better characteristics of the two: an external quantum efficiency (EQE) of 10.28% at 100 cd/m^2 and 7.12% at 1000 cd/m^2. Whereas the 5% loaded device demonstrated an EQE of 3.01% at 100 cd/m^2 but did not reach 1000 cd/m^2 brightness. This shows that the charge dynamics improve at higher loading due to better injection of electrons directly onto the **CT state**, see current density vs voltage characteristics in Figure 1a. Increasing the dopant concentration has previously been shown to improve the performance of phosphorescent devices.[21] The PLQY of 30% **2d**:TAPC is 53 ± 4% and that of 7% **2d**:TAPC is 50 ± 4%, equivalent within error limits. Very unusually (the presence of oxygen, and/or TF might explain this discrepancy), these values are far higher than **2d** in toluene solution (26%)[16a] and pure **2d** film (14%).

To estimate the efficiency of triplet harvesting in these devices, we assume the well known equation for the external quantum efficiency of an OLED;

$$\mathrm{EQE} = \eta_{\mathrm{out}}\,\eta_{\mathrm{fl}}\,\gamma\,\eta_{\mathrm{fr}} \quad (1)$$

where η_{out}, is the outcoupling factor taken at 30% maximum outcoupling efficiency,[22,23] η_{fl} the PLQY is 0.5 for the 30% **2d**:TAPC film, the charge balance factor, $\gamma = 1$, and only 25% singlet excitons are formed directly from charge recombination, η_{fr}, = 0.25, which contribute to emission. From this we estimate that the maximum possible external efficiency for our devices would be, $\mathrm{EQE}_{\mathrm{max}} \approx 1 \times 0.25 \times 0.5 \times 0.3 = 3.8\%$. With 30% **2d** loading, the highest device efficiency is 3.4 times greater (≈13.1% EQE at 20 cd/m^2). To achieve this we require η_{fr}= 0.85, implying almost 100% triplet harvesting and 50% internal quantum efficiency. Given the excellent agreement between PL

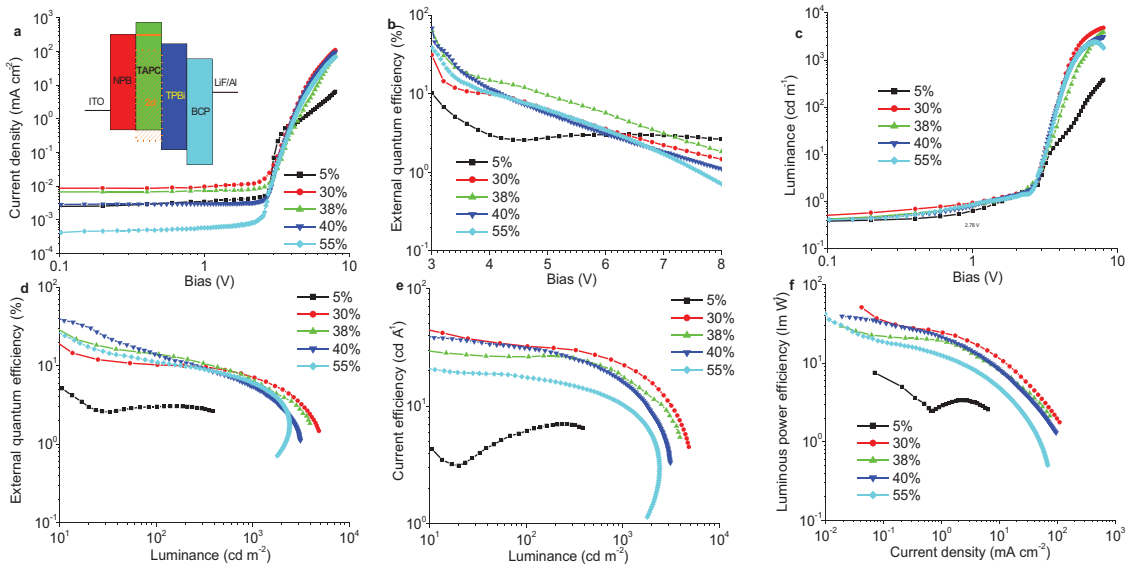

Figure 1. **2d**:TAPC OLED characteristics. a) Current density vs bias, b) EQE vs bias, c) luminance vs bias, d) EQE vs luminance, e) current efficiency vs luminance, f) power efficiency vs current density. The abnormally high EQE at very low brightness may be an artefact of making the measurement in a large 10 inch integrating sphere. Percentages of **2d** dopant, by weight, are indicated.

and EL spectra (see **Figure** 2b) in these devices and the 100% triplet conversion, we studied the detailed photophysics of the **2d**:TAPC system to elucidate the light generation mechanism.

2.2. Steady State Photophysics

The steady state PL from pure **2d** film, with λ_{max} = 450 nm, displays a small degree of charge transfer (CT) character; having a more gaussian band shape as opposed to a structured, local exciton (LE) band (Figure 2b).[10,16] As previously discussed, the excited states of molecules in the **2d** family, like all D–A systems have mixed CT+LE character wavefunctions and environment determines the exact nature of the final state.[16] The emission, in the solid state, is red-shifted by 50 nm in comparison with the PL of **2d** in hexane; the emission in this solvent has been assigned previously to LE emission as it shows weakly resolved vibronic structure.[16a] This red shift in film arises from the normal solid state packing effect, for example, see spectra in various environments presented elsewhere[26] for rubrene, and weak stabilization of CT via the low polarity (ground state) **2d** molecular environment. When doped into TAPC at 7% loading, the **2d** spectrum red-shifts to λ_{max} = 521 nm, broadens and gains substantial Gaussian band shape, characteristic of charge transfer excited state emission (Figure 2b). The PL spectrum of 30% **2d**:TAPC peaks at 540 nm and again has a Gaussian band shape. The EL spectra of 7% and 30% **2d** loading devices are identical to their respective PL spectra, which in itself is rather unusual. Thus, when **2d** is doped into TAPC the CT character of the excited state is stabilized. It is clear that the high device

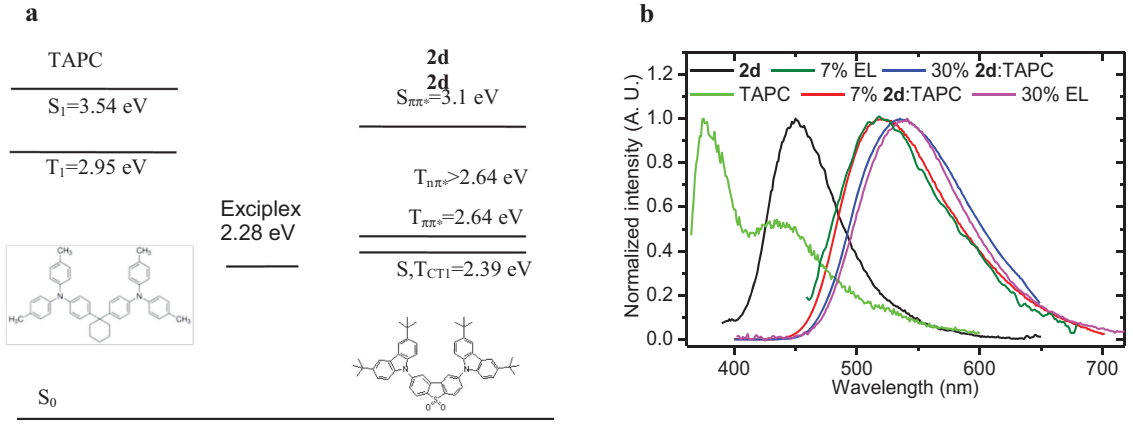

Figure 2. a) Structures and singlet, triplet levels of investigated molecules in the emitter layer. Triplet singlet levels of excitonic state have been taken as onsets from spectra from our measurements of **2d**:TAPC film for **2d** and literature for TAPC.[24,25] CT and exciplex energies are the average energy of the transition taken from the spectral peak position. b) Steady state PL spectra of **2d** and TAPC neat films and **2d** in TAPC at 7% and 30% loading. TAPC film PL:λ_{max} = 371 nm and TAPC excimer/dimer: λ_{max} = 468 nm.

efficiency correlates with the CT nature of the emitting species. In all cases, the on-set, or maximium energy of the CT stabilized state lie just below that of the lowest energy LE (π–π^*) triplet state observed in **2d**, Figure S1 in Supporting Information. It should be noted that the phosphorescence observed at 80 ms has well resolved vibronic features, and is at the same energy as **2d** in solution and is characteristic of a localized (π–π^*) triplet state on a carbazole unit.[16a] From Figure 1e, we also see that the device efficiency roll off is rather small which we take to indicate that the excitation energy resides as separated e-h charge pairs (the CT state) rather than excitons, and so are more stable with respect to polaron (charge) quenching, which is a problem at higher brightness with long lived excitations in Pt or Ir based phosphorescent complex emitters. It is obvious from TADF device results in general that the EL quenching mechanisms are a topic that needs to be revisited.

2.3. Delayed Fluorescence Dependence on Laser Fluence

To assign the origin of the delayed fluorescence (DF) emission we turned to time resolved emission spectroscopy (**Figure 3**). DF spectra of **2d**, 7% **2d**:TAPC and 30% **2d**:TAPC films (Figure 3a,b) have been recorded at different laser fluences. DF spectra has been recorded 100 ns after excitation with 1 ms integration window using gated iCCD camera. At (low) < 4 μJ excitation pulse energy, **2d** films emit a broad spectrum peaking at 520 nm which can be assigned to an ICT state emission.[16a] As laser fluence is increased, a new band peaking at ≈ 460 nm starts to rise on the blue edge of this band. This corresponds to the predominantly LE emission from **2d**, arising from TF.[16a,17] The DF spectrum of **2d** in TAPC is not dependent on laser fluence and peaks at ≈520 nm for 7% loading film and at ≈540 nm for 30% loading film (Figure 2b).

The DF emission intensity dependence on laser fluence from films was also measured (Figure 3c and Supporting Information Figure S2). DF emission intensity has been recorded 100 ns after excitation with 1 ms integration window using gated iCCD camera. DF emission from 7% **2d**:TAPC follows a power law with a slope approaching 1.09 in log–log scale (almost linear) independent of wavelength, and this clearly demonstrates that delayed emission in this sample is due to TADF[27] not TF (which would follow a quadratic power dependence). Similar dynamics (slope 0.87) have been observed in a 30% **2d** :TAPC film (Supporting Information, Figure S2). Interestingly, for the **2d** film, the intensity dependence on laser fluence on the red edge of the spectrum follows slope 1.04 identifying the TADF emission, and on the blue edge follows slope 1.87, which at high fluences turns to a linear dependency. The latter is characteristic behavior of the DF arising from TF and has been investigated many times previously in other systems.[28–30] The TF versus TADF interplay at different laser fluences in the delayed fluorescence in the **2d** films can be qualitatively explained in the following way. In a **2d** film molecules are "frozen" either in a more planar, LE, or more twisted, CT, molecular configuration. When laser fluence is low, both types of molecules are excited but the DF can arise only from the charge transfer molecules via TADF because the triplet exciton density is too low for the triplet annihilation to take place. As the laser fluence increases, the triplet annihilation rate increases due to higher triplet exciton densities and DF arises also through TF from the molecules that are "frozen" in the excitonic geometry. These observations point to a large morphological inhomogeneity in these materials, arising from the deposition method.

2.4. Photoluminescence Decays

The time resolved emission decays of **2d**, 7% **2d**:TAPC and 30% **2d**:TAPC films were studied and compared to that of **2d** in solution (Figure 3d). All of the decays have two "cascade" like features. In **2d** solution a clear distinction between PF and DF regimes is observed, both decaying in a monoexponential manner, with the former lasting up to 100 ns (monoexponential lifetime 5 ns) and the latter lasting from 400 ns to ≈1 ms, with DF/PF ratio of 0.048. Previously it has been determined that for **2d** in solution, the triplet yield is 5%[16a] indicating a DF yield is 100%, that is, 100% triplet harvesting. In film, the emission decay of **2d** changes, but the DF and PF are still distinguishable; however, neither PF nor DF follows monoexponential relationships, also the DF/PF ratio is higher than in the solution at 0.082, with the DF mainly due to TF at higher laser fluences as described above.

The contribution of DF increases substantially in **2d**:TAPC film where only TADF is responsible for the delayed emission. Substantial changes in the PF are also observed (Figure 3d and Supporting Information Figure S3). The PF of **2d** film (biexponential lifetimes of 1.6 ns and 5.5 ns), is rather similar to **2d** in solution (monoexponential lifetime 5 ns) whereas when doped in TAPC, the **2d** lifetime increases 80 fold; for the 7% **2d**:TAPC loading, the PL requires a triexponential fit over 7 orders of magnitude of time, with the shortest 'PF' lifetime of 393 ns and other components, 22 μs and 123 μs. This demonstrates a completely different origin of the initial decay component, and we ascribe this to the fact that no true PF occurs, instead all early time (0–400 ns) emission is TADF from a CT species. Previously[27] we have demonstrated that exciplexes can have long lifetimes in the range of 100 ns, through the recycling of triplet excitons between the near degenerate singlet and triplet CT levels. The temperature dependence of this early time component is very weak showing an initial small increase, followed by a small decrease with increasing temperature, mirroring a typical temperature dependence of the PLQY and indicative of near isoenergetic CT singlet and triplet levels (Figure 3e). Similarly the shortest lifetimes in 30% **2d**:TAPC are 47 ns and 429 ns (four exponentials fit over 7 orders of magnitude of time, other components are 18 μs and 44 μs), again showing the domination of the recycling process, excitation energy passing back and forth between the near isoenergetic ^{1}CT and ^{3}CT levels, giving rise to greatly extended lifetimes of the excited states.

DF and PF regimes are very difficult to distinguish in the **2d**:TAPC films and we evaluated that the DF/PF ratio reaches approximately 1.8 (7% **2d**) and 1.1 (30% **2d**). We further observe that the delayed component in the microseconds range increases strongly with increasing temperature (Figure 3e and Supporting Information Figure S4). This leaves no doubt that delayed fluorescence in **2d**:TAPC films arises from TADF. We

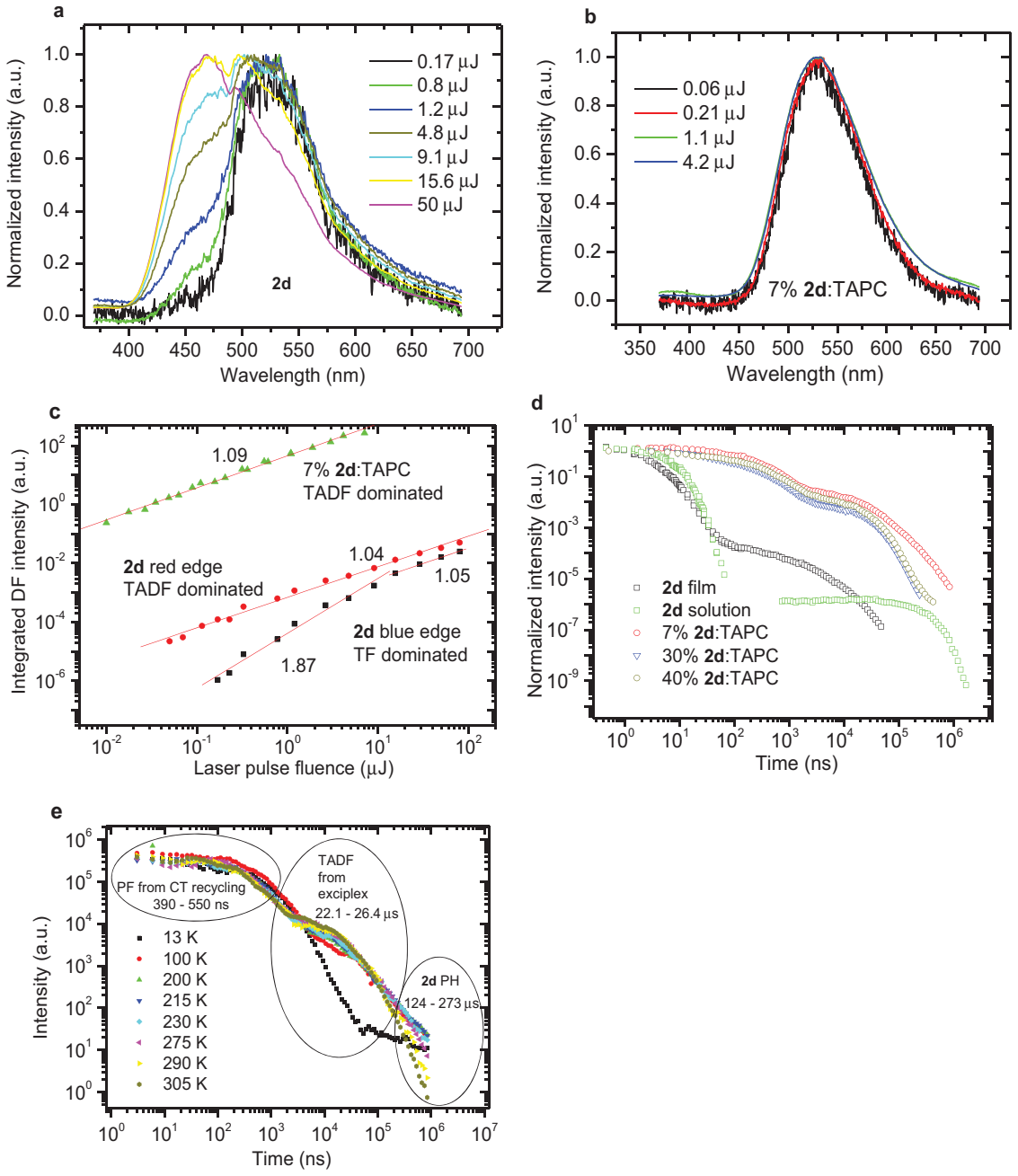

Figure 3. Normalized DF spectra (recorded >100 ns after excitation with gate iCCD camera) from **2d** film in a) and 7% **2d** : TAPC film in b). c) Dependence of delayed fluorescence intensity (peak emission) on laser pulse fluence (recorded >100 ns after excitation with gated iCCD camera). Numbers indicated are fitted slopes. Slope approaching 2 in log-log scale (quadratic law) indicates stronger TF influence for DF, and slope approaching 1 indicates stronger TADF influence to DF except when observed at high fluences. d) Decays of **2d** in solution, neat **2d**, 7% **2d**:TAPC, 30% **2d**:TAPC and 40% **2d**:TAPC films. e) Temperature dependence of 7% **2d**:TAPC decays. A tri-exponential equation was fitted in the temperature range from 305 K to 200 K. Three ranges can be distinguished at each temperature (lifetimes indicated on the curve, also in Table S1 in the Supporting Information). The shortest lifetime is ascribed to PF from singlet-triplet recycling within the CT states, the middle—to TADF from exciplex, and the longest—to phosphorescence.

ascribe this emission to come from a different CT state than that observed at early times. This will be described in detail in the next section. Unfortunately we cannot evaluate quantitatively the singlet triplet splitting of this new state due to the complicated and mixed decay dynamics in these films. However, we can qualitatively determine that the increase of the delayed component with increasing temperature is continuous from 14 K with no sudden step of DF (see Figure S4, Supporting Information), as we previously observed with **2d** in solution (from ≈240 K).[16a] This shows that the energy barrier for reverse intersystem crossing in both CT states, in the solid state, is much smaller than the activation energy of the ICT

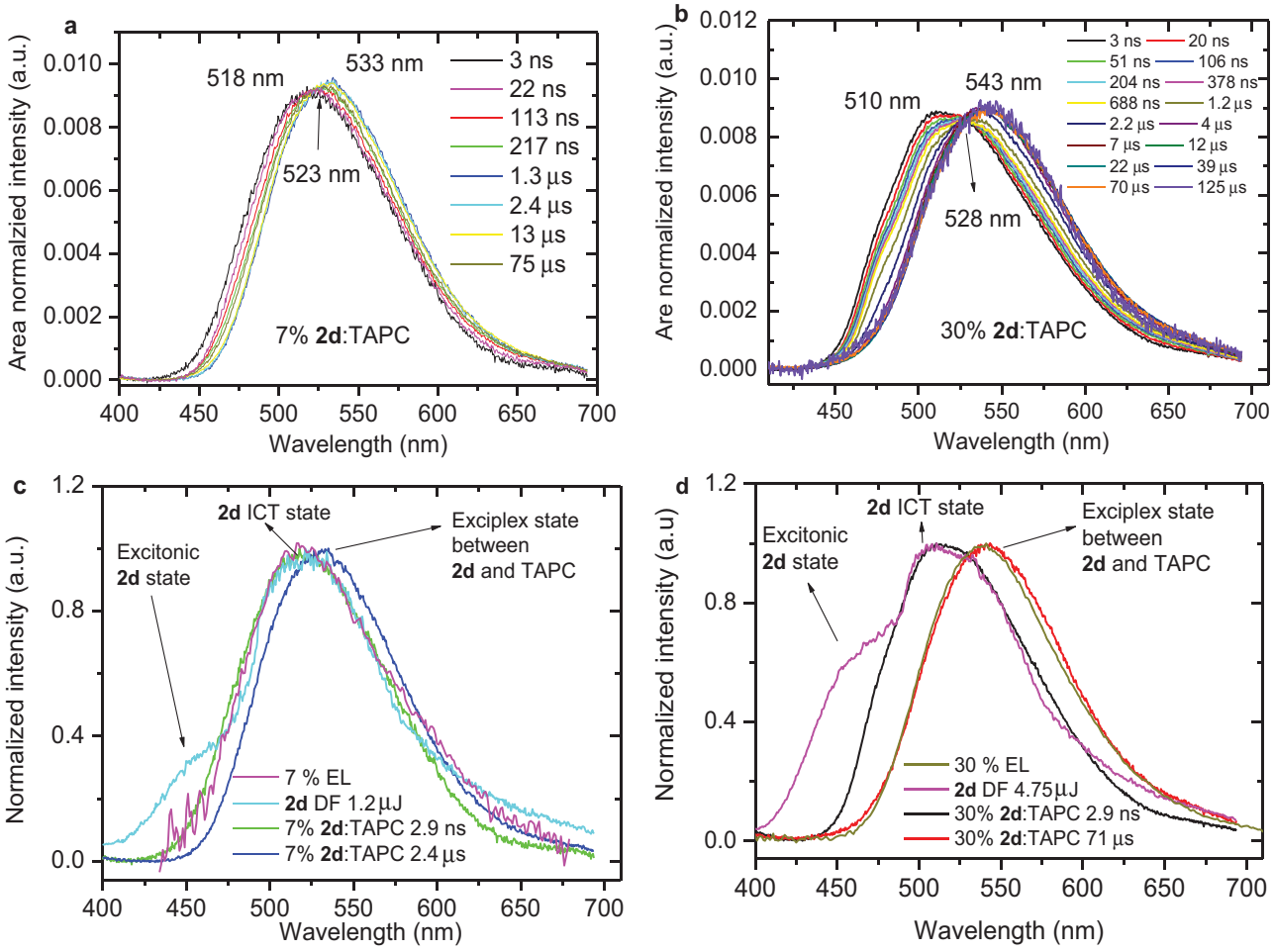

Figure 4. Time resolved area normalized spectra of a) 7% and b) 30% **2d**:TAPC. Isoemissive point is clearly visible in both samples. Time resolved normalized spectra of c) 7% and d) 30% **2d**:TAPC at early and at late times in comparison with DF spectrum of neat film, recorded 100 ns .. 1 ms at laser fluences indicated in the legends. EL spectra are added for comparison.

state of **2d** in solution, reported elsewhere[16a] (≈280 meV). This is in agreement with previous estimations of smaller singlet-triplet splitting in PBD:m-MTDATA exciplex (≈5 meV).[27]

2.5. Time Resolved Area Normalized Spectra

Time resolved area normalized analysis of the emission revealed the interplay between the two CT excited states in **2d**:TAPC films (**Figure 4**). An isoemissive point is clearly visible indicating that two species dominate the emission in these samples.[31] At early times (<1µs), in both doped samples, emission appears to be blue shifted with peaks at 510 nm (30% loading) and 518 nm (7% loading). We ascribe this early time "bluer" emission to the ICT state because this is identical to the DF spectra of pure **2d** film at low laser pump fluences which can only be assigned to ICT state emission (see Figure 4c and d). At later times in both samples a redder emission grows in at approximately 533 nm (7%) and 543 nm (30%). This emission has a pronounced Gaussian band shape and we therefore ascribe this to exciplex emission arising from an exciplex between **2d** and TAPC. Again, these observations fit well with the idea of a complex, heterogeneous molecular solid. Non-intuitively, steady state PL and EL spectra of 7% **2d**:TAPC coincide with the **2d** ICT emission spectrum; this shows the domination of **2d** ICT emission in low loaded films. Whereas, the steady state PL and EL spectra of 30% **2d**:TAPC coincide with the exciplex emission spectrum indicating that at higher loadings (near 1:2 molar mixtures of **2d** and TAPC), it is the exciplex species that dominates. It should be noted that time resolved spectra from 30% **2d**:TAPC film can be deconvoluted with two Gaussian bands corresponding to the ICT and exciplex emission features (Figure S5, Supporting Information). From this analysis it is clear that the two species are active in different time regimes, the ICT at early times, ca. the first 1–2 µs, and the exciplex from a few µs to several 100 µs. These two distinct time regimes are also clearly differentiated in the temperature behaviour of the DF as well, see Figure 3e, the ICT emission is virtually temperature independent indicative of near degenerate ^{1}CT and ^{3}CT levels, whereas the exciplex DF has a weak but clearly measurable temperature dependence which we estimate is due to a ^{1}CT-^{3}CT gap of > 5 meV.

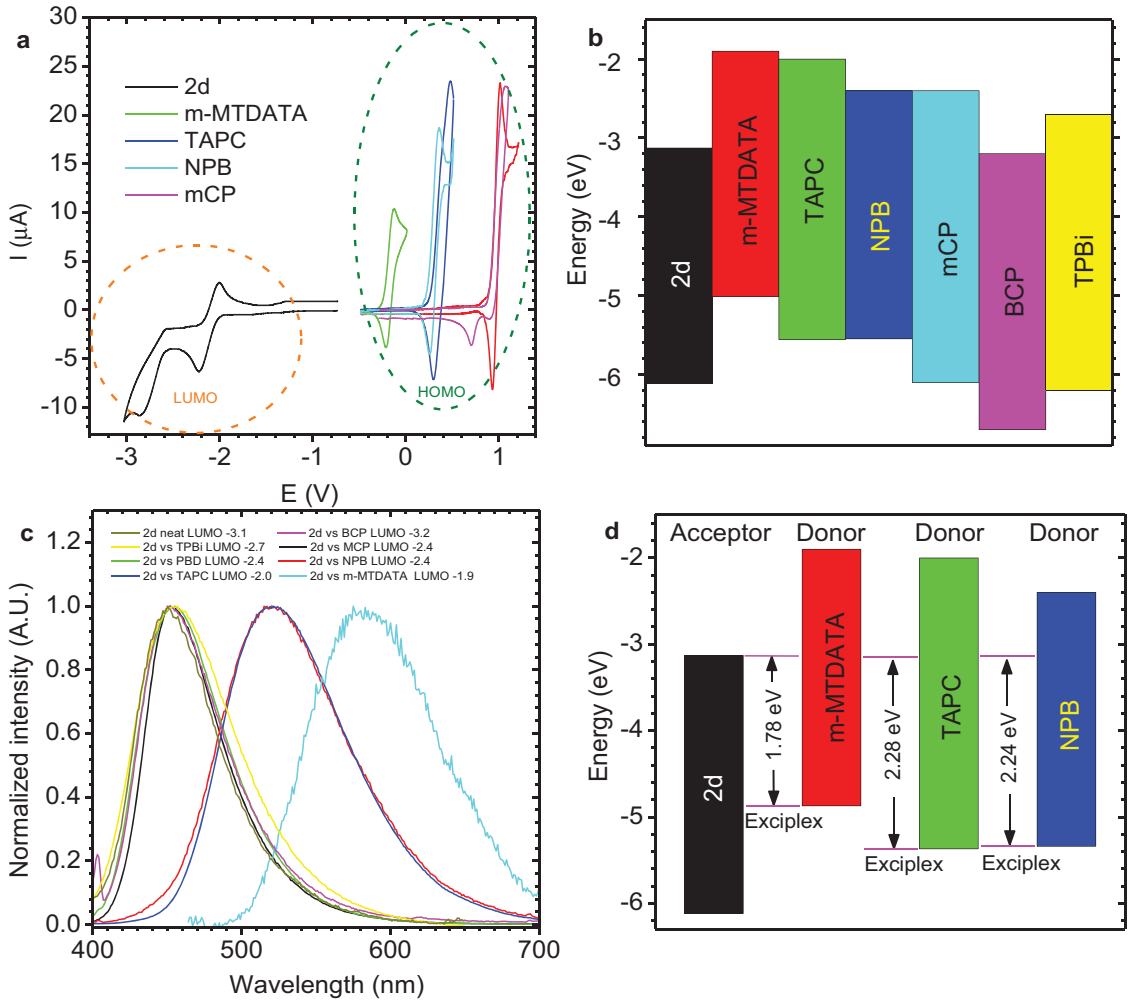

Figure 5. a) CV characteristics of **2d** and a small range of donnor molecules. b) The HOMO-LUMO levels determined from the redox levels of the molecules. c) Emission spectra of neat **2d** film and 50:50 mixtures of 2d and donor molecules, that clearly shows a diffferentiation between donors which can and those that cannot form an exciplex with **2d**. d) $HOMO_{don}$-$LUMO_{acc}$ levels and energy differences of the formed exciplexes.

We note that the PLQY of 7% and 30% **2d**:TAPC samples are very similar (≈50%) indicating that photophysically, ICT and exciplex states have similar oscillator strengths in this set of materials. However, in the case of **2d**:TAPC the exciplex is better for OLED devices, most probably due to enhanced charge balance and charge injection facilitated by the exciplex energy levels. This is reflected in the higher EQE in 30% **2d**:TAPC device. We note that the 40% **2d**:TAPC films show even more complex behavior with a continuous increase in exciplex contribution as time increases, see Supporting Information (Figure S6), and yields the most efficient devices.

2.6. Exciplex Formation

To confirm the exciplex formation between **2d** and TAPC, **2d** was mixed with various hosts having different HOMO-LUMO levels. The HOMO-LUMO levels were determined electrochemically (**Figure 5**a), using cyclic voltammetry (CV) analysis.[32] The values of the electron affinity and the ionization potential determined electrochemically are similar to the HOMO and LUMO energies determined spectroscopically (Figure 5b).[33]

Exciplex formation requires a charge transfer from the donor to the acceptor (or visa versa), and this requires considerable off-set between the LUMO levels of the donor and acceptor. We find that an offset >0.5 eV, higher donor LUMO compared to the acceptor LUMO, is required for the electron transfer to occur in the **2d** based systems (Figure S7, Supporting Information). Only when **2d** is mixed with materials having a higher LUMO by at least 0.5 eV and a higher HOMO by roughly the same energy off-set, is a red-shifted Gaussian-like exciplex emission observed, otherwise only acceptor (**2d**) emission is observed (Figure 5c). This is a more strict criterion for the formation of an exciplex state. Furthermore, a more important observation can be made, that the peak emission energies of the exciplexes with **2d** observed here are higher in energy than the difference between the donor oxidation (E_D^{ox}) and acceptor reduction (E_A^{red}) potential, that is, greater than the $LUMO_{acc}$–$HOMO_{don}$ gap. Following the analysis of exciplex energies (E_e) by Weller[12b] for the case of a true exciplex state

$$E_e = E_D^{ox} - E_A^{red} + U_{dest} - U_{stab} - \Delta H_e^{sol} + 0.32\text{eV} \quad (2)$$

For an exciplex U_{dest} and $U_{stab} \approx 0$, that is, the stabilization and destabilization effects of exciplex formation cancel. The energy gain due to the solubilisation of the transferred electron must be nearly zero in solid state, unless the dielectric constant of the host is very high. From the **2d** exciplex data we see that for **2d**:m-MTDATA, $h\nu_{max}$ is 0.34 eV greater than $E_D^{ox} - E_A^{red}$, whereas both **2d**:TAPC and **2d**:NPB are about 0.14 eV greater. In the latter cases this could imply either some degree of relaxation of the accepter on charge transfer, or the degree of charge transfer is less than 0.5.[12b] For **2d**:m-MTDATA, the fit to Equation 2 is excellent and is indicative of an exciplex with a degree of charge transfer 0.5 (half way between a heteroexcimer and a full ion pair state). These exciplexes should therefore have strongly mixed LE and CT character and thus have good PLQY.

3. Conclusion

In summary, we have shown that D–A molecules in the solid state can emit not only via intramolecular charge transfer excited states but also from exciplex states formed between the D–A molecules and a host. OLEDs based on our D–A–D molecule, **2d**, in TAPC host show nearly 100% efficient triplet harvesting and nearly 50% internal quantum yield, matching the PLQY, 53%, of the emitting state. This high efficiency achieved in these devices is unambiguously determined to come from triplet states which are harvested via thermally assisted delayed fluorescence, confirming this to be a very promising triplet harvesting method in OLEDs. Detailed photophysical studies reveal the complexity of the emission processes. In the same emissive molecule and host (both having high triplet levels) the emissive species depends critically on the concentration ratio of the two and the time after excitation, either an ICT state of the **2d** dopant or an exciplex state between the dopant and the host dominate the emission. With this set of materials the exciplex channel (at least 30% **2d** :TAPC) is preferred as this gives much higher device EQE, due to better injection and balanced charge transport. In this case we have demonstrated TADF OLEDs that reach EQE values of >14%, with emitters having a PLQY of ≈53%. From these measurements it is clear that very careful design of the TADF emission layer is needed to achieve the desired device performance. Clearly there must be a competition between ICT and exciplex formation, governed by the heterogeneous nature of the films. Also we find that a host acceptor that is able to give a ≈0.5 eV driving force is required to stabilize the exciplex formation, which is desirable in this materials set as the devices clearly have better electrical performance and also that these **2d** exciplexes follow Wellers empirical description such that the peak exciplex emission energy is ≈ 0.14 to 0.32 eV > $E_D^{ox} - E_A^{red}$, that is, greater than the $LUMO_{acc}$–$HOMO_{don}$ gap.

4. Experimental Section

OLED devices were fabricated using pre-cleaned indium-tin-oxide (ITO) coated glass substrates purchased from Ossila with a sheet resistance of 20 Ω/cm^2 and ITO thickness of 100 nm. The OLED devices had a pixel size of 2 mm by 1.5 mm. The small molecule and cathode layers were thermally evaporated using the Kurt J. Lesker Spectros II deposition chamber at 10^{-6} mbar. All organic materials and aluminium were deposited at a rate of 1 Å/s, the **2d**:TAPC layers were deposited between 0.4–2 Å/s (depending on the **2d** concentration), the LiF layer were deposited at 0.1 Å/s.

Thin film (deposition) thickness was re-measured using a J A Woolam VASE Ellipsometer. Both steady state absorption and emission were measured using commercially available machines, UV-3600 Shimadzu spectrophotometer and Jobin Yvon Horiba Fluoromax 3 or Fluorlog, respectively. Film photoluminescence quantum yield was measured as in the literature.[34] Spectra were corrected for system spectral response. Time resolved spectra were obtained by exciting the sample with a 150 ps-pulsed, 10 Hz, 355 nm Nd:YAG laser (EKSPLA). Sample emission was directed onto a spectrograph and gated iCCD camera (Stanford Computer Optics). PL decay transients were obtained using exponentially increasing decay and integration times, as previously described.[35]

Electrochemical measurements were carried out using standard potentiostat and cyclic voltammetry techniques. The electrochemical cell comprised a platinum disk with 1-mm working area diameter as the working electrode, a Ag/AgCl reference electrode and a platinum wire auxiliary electrode. Measurements were performed in 1.0 mM concentrations of all compounds in 0.1 M solutions of Bu_4NBF_4, 99% (TCI Chemicals) in dichloromethane (for oxidation) and tetrahydrofuran (for reduction) as solvents (CHROMASOLV, 99.9%, Sigma Aldrich) at room temperature. Cyclic voltamperometric measurements were conducted at room temperature under an argon atmosphere and at scan rate of 50 mV/s. All redox potentials are reported with the ferrocene/ferrocenium (Fc/Fc^+) redox couple as an internal reference system: 0.00 V.

The molecules investigated have a wide HOMO-LUMO gap which necessitated the use of different solvents: THF for reduction down to –3.5 V and DCM for oxidation up to +2.0 V (Figure 5a). Analysis of the data gave the relative energy plot (Figure 5b).

Supporting Information

Supporting Information is available from the Wiley Online Library or from the author.

Acknowledgements

P.D. acknowledges support from the Mobility Plus project financed by the Polish Ministry of Science and Higher Education. The authors thank EPSRC for funding. Figure 3e was corrected on October 15, 2014.

Received: March 24, 2014
Revised: June 15, 2014
Published online: August 8, 2014

[1] D. Y. Kondakov, *J. Appl. Phys.* **2007**, *102*, 114504.
[2] V. Adamovich, J. Brooks, A. Tamayo, A. M. Alexander, P. I. Djurovich, B. W. D'Andrade, C. Adachi, S. R. Forrest, M. E. Thompson, *New J. Chem.* **2002**, *26*, 1171.
[3] Y. Sun, S. R. Forrest, *Appl. Phys. Lett.* **2007**, *91*, 263503.
[4] C. Adachi, M. A. Baldo, M. E. Thompson, S. R. Forrest, *J. Appl. Phys.* **2001**, *90*, 5048.
[5] L. R. Lakowicz, *Principles of Fluorescence Spectroscopy* Kluwer Academic/Plenum Pyblishers, New York **1999**.
[6] V. Sivasubramaniam, F. Brodkorb, S. Hanning, H. P. Loebl, V. van Elsbergen, H. Boerner, U. Scherf, M. Kreyenschmidt, *J. Fluorine Chem.* **2009**, *130*, 640.

[7] D. Y. Kondakov, T. D. Pawlik, T. K. Hatwar, J. P. Spindler, *J. Appl. Phys.* **2009**, *106*, 124510.
[8] S. M. King, M. Cass, M. Pintani, C. Coward, F. B. Dias, A. P. Monkman, M. Roberts, *J. Appl. Phys.* **2011**, *109*, 074502.
[9] Y. Zhang, S. R. Forrest, *Phys. Rev. Lett.* **2012**, *108*, 267404.
[10] K. Goushi, K. Yoshida, K. Sato, C. Adachi, *Nat. Photonics* **2012**, *6*, 253.
[11] S. Y. Lee, T. Yasuda, H. Nomura, C. Adachi, *Appl. Phys. Lett.* **2012**, 101.
[12] a)H. Beens, A. Weller, *Acta Phys. Polonica* **1968**, *34*, 539; b)A. Weller in *The Exciplex* (Eds: M. Gordon, W. R. Ware), Academic Press Inc., London **1975**.
[13] B. Frederichs, H. Staerk, *Chem. Phys. Lett.* **2008**, *460*, 116.
[14] H. Uoyama, K. Goushi, K. Shizu, H. Nomura, C. Adachi, *Nature* **2012**, *492*, 234.
[15] K. Sato, K. Shizu, K. Yoshimura, A. Kawada, H. Miyazaki, C. Adachi, *Phys. Rev. Lett.* **2013**, *110*, 247401.
[16] a)F. B. Dias, K. N. Bourdakos, V. Jankus, K. C. Moss, K. T. Kamtekar, V. Bhalla, J. Santos, M. R. Bryce, A. P. Monkman, *Adv. Mater.* **2013**, *25*, 3707; b)K. C. Moss, K. N. Bourdakos, V. Bhalla, K. T. Kamtekar, M. R. Bryce, M. A. Fox, H. L. Vaughan, F. B. Dias, A. P. Monkman, *J. Organ. Chem.* **2010**, *75*, 6771; c)F. B Dias, S. Pollock, G. Hedley, L.-O. Palsson, A. Monkman, I. I. Perepichka, I. F. Perepichka, M. Tavasli, M. R Bryce, *J. Phys. Chem B* **2006**, *110*, 19329.
[17] V. Jankus, C.-J. Chiang, F. Dias, A. P. Monkman, *Adv. Mater.* **2013**, *25*, 1455.
[18] K. T. Kamtekar, K. Dahms, A. S. Batsanov, V. Jankus, H. L. Vaughan, A. P. Monkman, M. R. Bryce, *J. Polym. Sci. Part A* **2010**, *49*, 1129.
[19] Y. Zheng, A. S. Batsanov, V. Jankus, F. B. Dias, M. R. Bryce, A. P. Monkman, *J. Organ. Chem.* **2011**, *76*, 8300.
[20] B. S. Mashford, M. Stevenson, Z. Popovic, C. Hamilton, Z. Zhou, C. Breen, J. Steckel, V. Bulovic, M. Bawendi, S. Coe-Sullivan, P. T. Kazlas, *Nat. Photonics* **2013**, *7*, 407.
[21] V. N. Kozhevnikov, Y. Zheng, M. Clough, H. A. Al-Attar, G. C. Griffiths, K. Abdullah, S. Raisys, V. Jankus, M. R. Bryce, A. P. Monkman, *Chem. Mater.* **2013**, *25*, 2352.
[22] M. Furno, R. Meerheim, S. Hofmann, B. Luessem, K. Leo, *Phys. Rev. B* **2012**, 85.
[23] N. C. Greenham, R. H. Friend, D. D. C. Bradley, *Adv. Mater.* **1994**, *6*, 491.
[24] K. Goushi, R. Kwong, J. J. Brown, H. Sasabe, C. Adachi, *J. Appl. Phys.* **2004**, *95*, 7798.
[25] S.-y. Takizawa, V. A. Montes, P. Anzenbacher, *Chem. Mater.* **2009**, *21*, 2452.
[26] V. Jankus, E. W. Snedden, D. W. Bright, E. Arac, D. Dai, A. P. Monkman, *Phys. Rev. B* **2013**, *87*, 224202.
[27] D. Graves, V. Jankus, F. B. Dias, A. Monkman, *Adv. Funct. Mater.* **2014**, *24*, 2343.
[28] D. Hertel, H. Bassler, R. Guentner, U. Scherf, *J. Chem. Phys.* **2001**, *115*, 10007.
[29] V. Jankus, E. W. Snedden, D. W. Bright, V. L. Whittle, J. A. G. Williams, A. Monkman, *Adv. Funct. Mater.* **2013**, *23*, 384.
[30] T. N. Singh-Rachford, F. N. Castellano, *Coordination Chem. Rev.* **2010**, *254*, 2560.
[31] A. S. R. Koti, M. M. G. Krishna, N. Periasamy, *J. Phys. Chem. A* **2001**, *105*, 1767.
[32] P. Data, P. Pander, M. Lapkowski, A. Swist, J. Soloducho, R. R. Reghu, J. V. Grazulevicius, *Electrochim. Acta* **2014**, 128, 430.
[33] J.-L. Bredas, *Mater. Horizons* **2014**, *1*, 17.
[34] L.-O. Palsson, A. P. Monkman, *Adv. Mater.* **2002**, *14*, 757.
[35] C. Rothe, A. P. Monkman, *Phys. Rev. B* **2003**, *68*, 075208.